Probabilistic assessment of hydrologic retention performance of green roof considering aleatory and epistemic uncertainties

Lingwan You, Yeou-Koung Tung and Chulsang Yoo

ABSTRACT

Green roofs (GRs) are well known for source control of runoff quantity in sustainable urban stormwater management. By considering the inherent randomness of rainfall characteristics, this study derives the probability distribution of rainfall retention ratio R_r and its statistical moments. The distribution function of R_r can be used to establish a unique relationship between target retention ratio $R_{r,T}$, achievable reliability AR, and substrate depth h for the aleatory-based probabilistic (AP) GR design. However, uncertainties of epistemic nature also exist in the AP GR model that makes AR uncertain. In the paper, the treatment of epistemic uncertainty in the AP GR model is presented and implemented for the uncertainty quantification of AR. It is shown that design without considering epistemic uncertainties by the AP GR model yields about 50% confidence of meeting $R_{r,T}$. A procedure is presented to determine the design substrate depth having the stipulated confidence to satisfy $R_{r,T}$ and target achievable reliability AR_T.

Key words | green roof, probabilistic-based design, probability, retention ratio, uncertainty analysis

Lingwan You (corresponding author)
Yeou-Koung Tung
Disaster Prevention and Water Environment Research Center,
National Chiao Tung University,
Hsinchu,
Taiwan
E-mail: *lucie751111@gmail.com*

Chulsang Yoo
Department of Civil, Environment, and Architecture,
Korea University,
Seoul,
South Korea

HIGHLIGHTS

- Derive the probability distribution of the rainfall retention ratio of green roof (GR) and its statistical moments.
- Present an aleatory-based probabilistic (AP) model for GR design.
- The paper shows that the design without considering epistemic uncertainties by the AP GR model yields about 50% confidence of meeting target retention ratio.
- Propose a methodology to treat epistemic uncertainty in the AP model for the uncertainty quantification of achievable reliability.
- Demonstrate the analysis procedures *via* a numerical example to determine GR substrate depth having the stipulated confidence to satisfy target retention ratio and target reliability.

INTRODUCTION

The use of green roofs (GRs) is becoming popular in sustainable urban stormwater management. Contributions of GRs to urban runoff control and management are primarily attributed to their retention and detention abilities, which not only reduce runoff volume but also delay and attenuate runoff peak discharge (Berndtsson 2010; Mobilia *et al.* 2015; Stovin *et al.* 2017). Other than the advantages in the hydrologic aspect, GRs can improve biodiversity in urban areas,

doi: 10.2166/nh.2020.086

enhance urban runoff water quality, moderate heat island effect, improve building energy efficiency, remove pollutants in the air, and increase the life expectancy of building roof systems (Vijayaraghavan 2016).

Evaluations of the hydrologic performance of GRs have been made by field monitoring of prototype or laboratory-scale facilities over a selected period of time (e.g., Carter & Rasmussen 2006; Getter *et al.* 2007; Soulis *et al.* 2017; Johannessen *et al.* 2018). Also, a commonly seen approach is the use of the model of various types to evaluate hydrologic performance by simulating the runoff response of a schematized GR system under different rainfall conditions (Li & Babcock 2014; Ercolani *et al.* 2018; Mora-Melià *et al.* 2018). Depending on the performance indicators of interest, the complexity of the modeling tool may vary (Mobilia *et al.* 2015). To assess detention performance, one would use a physical-based hydrologic/hydraulic model that can produce time-varying runoff hydrographs from the GRs. For retention evaluation, a simple lumped hydrologic model considering event-based water balance (Carter & Jackson 2007; Starry *et al.* 2016; Chai *et al.* 2017) would generally be sufficient.

A commonly used hydrologic indicator for GR's retention performance is the rainfall retention ratio R_r:

$$R_r = \frac{v - v_{rg}}{v} = 1 - \frac{v_{rg}}{v} \tag{1}$$

in which v, v_{rg} are the rainfall amount and the corresponding runoff volume from a GR system, respectively. The complimentary performance indicator to retention ratio R_r is the runoff production ratio R_p:

$$R_p = \frac{v_{rg}}{v} = 1 - R_r \tag{2}$$

From the runoff control viewpoint, a GR system with a lower runoff production ratio or higher rainfall retention ratio is more desirable.

Basic GR hydrologic model

As the focus of performance herein is hydrologic retention, a simple lumped water balance model (Zhang & Guo 2013) for a GR system is adopted:

$$R_c = S_l + S_c + (\theta_{fc} - \theta_i)h \tag{3}$$

where R_c is the retention capacity of the GR system; S_l is the interception by plants; S_c is the capacity of the storage layer; θ_{fc} is the field capacity of the substrate; θ_i is the initial soil moisture content at the beginning of each rainstorm event; h is the depth of the substrate. The term, $(\theta_{fc} - \theta_i)h$, in Equation (3) is the available water holding capacity (*WHC*) in the substrate during a rainstorm event (Allen *et al.* 1998; Fassman & Simcock 2012). Assuming the substrate is maintained above the plant's wilting point, θ_{wp}, the GR system reaches its maximum retention capacity $R_{c,\max}$ when $\theta_i = \theta_{wp}$ as:

$$R_{c,\max} = S_l + S_c + (\theta_{fc} - \theta_{wp})h \tag{4}$$

The term $(\theta_{fc} - \theta_{wp})h$ is the maximum *WHC* of the substrate.

The initial soil moisture θ_i at the beginning of a rainfall event depends on the length of antecedence dry period b, evapotranspiration (ET) rate E_a, and evapotranspirable water content W_i in the GR system at the end of the preceding rainfall event. The runoff volume from a GR system can be obtained as (Zhang & Guo 2013):

$$v_{rg} = \begin{cases} 0, & \left[v \le R_{c,\max},\ b > \frac{W_i}{E_a}\right] \text{ or } \left[v \le R_{c,\max} - W_i + E_a b,\ b \le \frac{W_i}{E_a}\right] \\ v + W_i - R_{c,\max} - E_a b, & \left[v > R_{c,\max} - W_i + E_a b,\ b \le \frac{W_i}{E_a}\right] \\ v - R_{c,\max}, & \left[v > R_{c,\max},\ b > \frac{W_i}{E_a}\right] \end{cases} \tag{5}$$

From Equation (5), one is able to determine runoff volume v_{rg} from which the GR retention ratio can be calculated by Equation (1).

Uncertainties in GR performance evaluation

Referring to Equation (5), hydrologic retention assessment of a GR system involves uncertainties from various sources, which can be generally categorized into two types: aleatory and epistemic uncertainties. The former is due to the inherent natural randomness of rainfall events such as rainfall depth, duration, inter-event dry period, and temporal pattern. On the other hand, epistemic uncertainties arise from knowledge insufficiency about the rainfall-runoff transformation process in GR systems (i.e., the model), and lack of complete characterization of model parameters associated with the soil-plant-climatic system. Therefore, the assessment of the performance of a GR system in reality cannot be certain. It would be desirable to quantify the uncertainty features of the performance indicators as affected by various sources of uncertainty so that a more comprehensive analysis and design of GR systems can be made.

Probabilistic modeling of a GR system can be approached in two ways. One is an implicit approach by which a deterministic model describing involved hydrologic/hydraulic processes is coupled with long-term historically observed or stochastically synthesized climatic inputs to generate plausible realizations of the system outputs (Carson *et al.* 2013; Stovin *et al.* 2013; Locatelli *et al.* 2014; Cipolla *et al.* 2016; Chow *et al.* 2017). The alternative is an explicit approach to analytically derive the probabilistic features of the system performance indicators (e.g., retention ratio) for a GR system (Zhang & Guo 2013; Guo *et al.* 2014; Guo 2016). The implicit approach has the advantage of being able to preserve the physical features of involved processes more fully, but it is more computationally intensive. The explicit approach can provide a direct assessment of the uncertainty features of the system performance without extensive simulation, but more simplifications and idealizations of the system behaviors might be required.

Note that R_r and R_p in Equation (2) are functions of rainfall amount and the corresponding runoff volume produced which, in turn, is affected by rainstorm inter-event dry period and properties of substrate (e.g., depth, porosity, and hydraulic conductivity) and vegetation (e.g., plant type and ET). Many of these factors affecting retention (or runoff production) ratio are subject to uncertainties. Specifically, uncertainties associated with rainfall amount and the inter-event time of storm are of aleatory nature, whereas uncertainties corresponding to model parameters defining the properties of substrate, vegetation, and climate are of epistemic type. The importance of incorporating both aleatory and epistemic uncertainties in reliability evaluation has been elaborated in groundwater remediation (Hora 1996), structural systems (Der Kiureghian & Ditlevsen 2009), seismic modeling (Lambardi 2017), and detention basin capacity determination (Tung 2017).

Outline of the study

The overall probabilistic analysis of GR retention performance presented herein consists of two stages (see Figure 1). Stage-I, described in the 'AP GR Model' section, treats aleatory uncertainty from the randomness of rainfall properties. Based on the probability distribution of the GR runoff volume derived by Zhang & Guo (2013), close-form expressions for the probability distribution of retention ratio R_r from which the corresponding statistical moments are derived. This probability distribution of R_r can be used for the design of the GR system considering the reliability of achieving target retention ratio. Stage-II, described in the 'Incorporating Epistemic Uncertainty in the AP GR Model' section, further deals with epistemic uncertainties associated with the model parameters. Uncertainty features associated with the aleatory-based probabilistic (AP) GR model are quantified for assessing the confidence of meeting the target retention ratio and target achievable reliability. Through a numerical example, the 'Illustration' section demonstrates the probabilistic behaviors of retention ratio for a GR system and the relations between achievable reliability with substrate depth (Stage-I). Moreover, a method to systematically evaluate the statistical properties of the AP GR model considering epistemic uncertainty is presented (Stage-II). Through uncertainty analysis (UA), a reliability-based design of substrate depth for the GR system with a specific confidence of meeting target retention ratio $R_{r,T}$ and achievable reliability AR_T can be implemented.

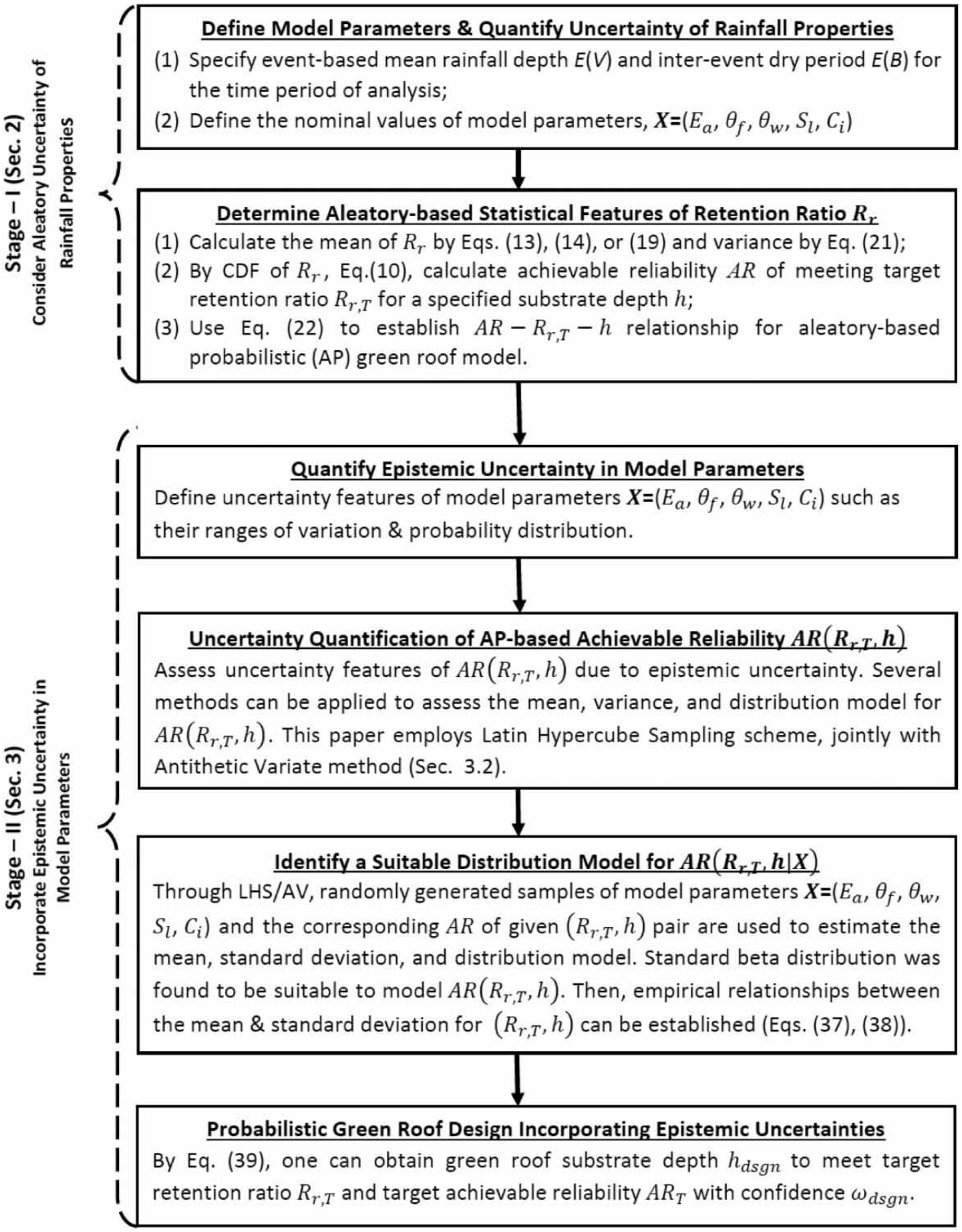

Figure 1 | Outline of the probabilistic analysis/design procedure for extensive GRs.

AP GR MODEL

Consider the aleatory uncertainty due to the natural randomness of rainfall amount V and inter-event dry period B. By taking these two rainfall properties to be statistically independent random variables, each, respectively, has an exponential distribution with the probability density functions (PDFs) defined as:

$$\text{Rainfall volume } (V)\text{: } f_V(v) = \zeta e^{-\zeta v}, \quad v \geq 0 \tag{6}$$

$$\text{Inter-event dry time } (B)\text{: } f_B(b) = \psi e^{-\psi b}, \quad b \geq 0 \tag{7}$$

in which $\zeta = 1/\mu_V$ and $\psi = 1/\mu_B$ are, respectively, exponential distribution parameters relating to the mean values of random rainfall depth μ_V and inter-event dry period μ_B. Verifications and justifications of exponential distribution models for V and B of individual storm event can be found in numerous analysis of rainfall data (e.g., Eagleson 1978; Adams et al. 1986; Guo & Adams 1998; Guo 2001; Guo & Baetz 2007).

Based on Equation (5), along with exponential distributions for rainfall properties, Equations (6) and (7), Zhang & Guo (2013) derived the cumulative distribution function (CDF) and PDF of the GR runoff volume V_{rg} as functions of the rainfall distribution parameters ζ and ψ as:

$$\text{CDF: } F_{V_{rg}}(v_{rg}) = Pr(V_{rg} \le v_{rg}) = 1 - \frac{e^{-\zeta(v_{rg}+R_{c,\max})}}{\psi + \zeta E_a}(\psi e^{\zeta W_i} + \zeta E_a e^{-(\psi W_i/E_a)}) \text{ for } v_{rg} \ge 0 \tag{8}$$

$$\text{PDF: } f_{V_{rg}}(v_{rg}) = \begin{cases} 1 - \dfrac{e^{-\zeta R_{c,\max}}}{\psi+\zeta E_a}(\psi e^{\zeta W_i} + \zeta E_a e^{-(\psi W_i/E_a)}), & v_{rg} = 0 \\ \dfrac{\zeta e^{-\zeta(v_{rg}+R_{c,\max})}}{\psi+\zeta E_a}(\psi e^{\zeta W_i} + \zeta E_a e^{-(\psi W_i/E_a)}), & v_{rg} > 0 \end{cases} \tag{9}$$

where $F_{V_{rg}}(\cdot)$ and $f_{V_{rg}}(\cdot)$ are, respectively, the CDF and PDF of the GR runoff volume.

Probability distribution of rainfall retention ratio

Based on the CDF and PDF of V_{rg} given in Equations (8) and (9), this section presents the distribution functions of retention ratio R_r as:

$$F_{R_r}(\eta') = e^{-((\psi W_i/E_a)+(\zeta R_{c,\max}/\eta'))} + \left(\frac{\psi}{\psi + (\zeta E_a/\eta')}\right)[e^{-(\zeta(R_{c,\max}-W_i)/\eta')} - e^{-((\zeta R_{c,\max}/\eta')+(\psi W_i/E_a))}] \tag{10}$$

where $F_{R_r}(\cdot)$, $f_{R_r}(\cdot)$ are the CDF and PDF of R_r, respectively; η' is the dummy variable; and $Pr(V_{rg} = 0)$ is the probability that the GR system produces zero runoff, which can be determined by Equation (8) as:

$$Pr(V_{rg} = 0) = 1 - \frac{e^{-\zeta R_{c,\max}}}{\psi + \zeta E_a}(\psi e^{\zeta W_i} + \zeta E_a e^{-(\psi W_i/E_a)}) \tag{12}$$

A brief description of the mathematical derivation of the CDF and PDF of R_r is presented in the Appendix in Supplementary Materials.

Statistical moments of retention ratio

To estimate the mean retention ratio $E(R_r)$, a simple way is by the first-order linear approximation through which the mean values of rainfall amount and runoff volume are used as:

$$E(R_r) = 1 - E\left(\frac{V_{rg}}{V}\right) \cong 1 - \frac{E(V_{rg})}{E(V)} \tag{13}$$

in which $E(\cdot)$ is the statistical expectation operator. Note that the above approximation assumes that random rainfall amount and runoff volume are statistically independent. Since R_r is non-linearly related to rainfall amount V and runoff volume V_{rg}, and the latter is also affected by the former, this indicates that rainfall amount and runoff volume are correlated. However, the first-order linear approximation, given by Equation (13), does not account for dependence between rainfall amount and runoff volume. By considering the second-order approximation, $E(R_r)$ can be estimated by (Tung & Yen 2005):

$$E(R_r) \approx 1 - \frac{E(V_{rg})}{E(V)} + \frac{1}{E^2(V)}Cov(V_{rg}, V) - \frac{E(V_{rg})}{E^3(V)}Var(V) \tag{14}$$

$$f_{R_r}(\eta') = \begin{cases} \left(\dfrac{\zeta\, e^{-(\zeta R_{c,\max}/\eta')}}{\eta'^2}\right)\left\{ e^{-(\psi W_i/E_a)}\left[R_{c,\max} - \dfrac{\psi\, R_{c,\max}}{\psi + (\zeta E_a/\eta')} - \dfrac{\psi\, E_a}{(\psi + (\zeta E_a/\eta'))^2}\right] + \dfrac{\psi}{\psi + (\zeta E_a/\eta')} e^{\zeta W_i/\eta'}\left[\dfrac{E_a}{\psi + (\zeta E_a/\eta')} + R_{c,\max} - W_i\right]\right\}, & 0 \le \eta' < 1 \\ Pr(V_{rg} = 0), & \eta' = 1 \end{cases} \tag{11}$$

which shows that the information about the variance of rainfall amount and its correlation with the runoff volume, represented by $Cov(V_{rg}, V)$, also play a role in estimating $E(R_r)$. The covariance of V_{rg} and V can be obtained from:

$$Cov(V_{rg},\ V) = E(V_{rg}\ V) - E(V_{rg})E(V) \tag{15}$$

where $E(V) = 1/\zeta$ defined by Equation (6) and

$$\begin{aligned} E(V_{rg}\ V) &= \int_0^\infty \int_0^\infty v_{rg} v\, f(v_{rg}, v)\, dv_{rg}\, dv = \int_0^\infty \int_0^\infty [v_{rg}(v, b)v\ ]\, f_V(v) f_B(b)\, dv\, db \\ &= \left(\frac{\psi}{\psi + \zeta E_a}\right) e^{-\zeta(R_{c,\max} - W_i)} \left\{ \left(\frac{2 + \zeta(R_{c,\max} - W_i)}{\zeta^2} + \frac{E_a}{\zeta(\psi + \zeta E_a)}\right)(1 - e^{-(\zeta W_i + (\psi W_i/E_a))}) - \left(\frac{W_i}{\zeta}\right) e^{-(\zeta W_i + (\psi W_i/E_a))} \right\} \\ &+ \left(\frac{R_{c,\max}}{\zeta} + \frac{2}{\zeta^2}\right) e^{-(\zeta R_{c,\max} + (\psi W_i/E_a))} \end{aligned} \tag{16}$$

The mean runoff volume $E(V_{rg})$ in Equation (15) has been derived by Zhang & Guo (2013) as:

$$E(V_{rg}) = \int_0^\infty v_{rg} f_{V_{rg}}(v_{rg}) dv_{rg} = \frac{e^{-\zeta R_{c,\max}}}{\zeta(\psi + \zeta E_a)} (\psi e^{\zeta W_i} + \zeta E_a e^{-(\psi W_i/E_a)}) \tag{17}$$

From the PDF of R_r, Equation (11), the statistical moments of R_r of any order m can be presented by:

$$E[R_r^m] = \int_0^1 (\eta')^m f_{R_r}(\eta')\, d\eta', \qquad m = 1,\ 2,\ 3,\ \ldots \tag{18}$$

The analytical expression of $E(R_r)$ can be derived as:

$$\begin{aligned} E(R_r) =& - \mathbb{E}_1(\zeta R_{c,\max}) \left[\zeta R_{c,\max} \left(\frac{E_a}{\psi R_{c,\max}}\right)\right] e^{-(\psi W_i/E_a)} \\ &+ \mathbb{E}_1\left(\left(\zeta + \frac{\psi}{E_a}\right) R_{c,\max}\right) \left[\zeta R_{c,\max}\left(\frac{E_a}{\psi R_{c,\max}}\right)\right] e^{((\psi(R_{c,max} - W_i))/(E_a))} \\ &+ \mathbb{E}_1(\zeta(R_{c,\max} - W_i)) \left[\zeta(R_{c,\max} - W_i)\left(\frac{E_a}{\psi(R_{c,\max} - W_i)} + 1\right)\right] \\ &- \mathbb{E}_1\left(\left(\zeta + \frac{\psi}{E_a}\right)(R_{c,\max} - W_i)\right) \\ &\times \left[\zeta R_{c,\max}\left(\frac{E_a}{\psi R_{c,\max}}\right)\right] e^{((\psi(R_{c,\max} - W_i))/(E_a))} - e^{-\zeta(R_{c,\max} - W_i)} + 1 \end{aligned} \tag{19}$$

in which $\mathbb{E}_1(\theta)$ is the exponential integral defined as (Abramowitz & Stegun 1964):

$$\mathbb{E}_1(\theta) = \int_\theta^\infty \frac{e^{-t}}{t} dt \tag{20}$$

Similarly, the analytical expression for the variance of R_r can be obtained from $Var(R_r) = E[R_r^2] - E^2(R_r)$ in which,

For the skew coefficient of R_r, it can be derived from the third-order moment $E[R_r^3]$.

$$\begin{aligned} E[R_r^2] =& \mathbb{E}_1(\zeta R_{c,\max}) \left[2\zeta^2 R_{c,\max}^2 \left(\left(\frac{E_a}{\psi R_{c,\max}}\right)^2 + \frac{E_a}{\psi R_{c,\max}}\right)\right] e^{-(\psi W_i/E_a)} - \mathbb{E}_1\left(\left(\zeta + \frac{\psi}{E_a}\right) R_{c,\max}\right) \left[2\zeta^2 R_{c,\max}^2 \left(\frac{E_a}{\psi R}\right)^2\right] e^{\psi(R_{c,\max} - W_i)/E_a} \\ &- \mathbb{E}_1(\zeta(R_{c,\max} - W_i)) \left[\zeta^2 (R_{c,\max} - W_i)^2 \left(2\left(\frac{E_a}{\psi(R_{c,\max} - W_i)}\right)^2 + 2\frac{E_a}{\psi(R_{c,\max} - W_i)} + 1\right)\right] \\ &+ \mathbb{E}\left(\left(\zeta + \frac{\psi}{E_a}\right)(R_{c,\max} - W_i)\right) \left[2\zeta^2 R_{c,\max}^2 \left(\frac{E_a}{\psi R_{c,\max}}\right)^2\right] e^{\psi(R_{c,\max} - W_i)/E_a} - \left[2\zeta R_{c,\max}\left(\frac{E_a}{\psi R_{c,\max}}\right)\right] e^{-((\psi W_i/E_a) + \zeta R_{c,\max})} \\ &+ \left[\zeta(R_{c,\max} - W_i)\left(2\frac{E_a}{\psi(R_{c,\max} - W_i)} - \frac{1}{\zeta(R_{c,\max} - W_i)} + 1\right)\right] e^{-\zeta(R_{c,\max} - W_i)} + 1 \end{aligned} \tag{21}$$

AP GR design

To quantify the probabilistic performance of a GR system by solely considering aleatory uncertainty, achievable reliability is utilized herein as a performance indicator:

$$AR(R_{r,T};\ h) = Pr(R_r \geq R_{r,T};\ h) = 1 - F_{R_r}(R_{r,T};\ h) \quad (22)$$

where $AR(R_{r,T};\ h)$ is the achievable reliability of meeting the target retention ratio, $R_{r,T}$, conditioned on substrate depth, h. As shown in Equations (10) and (22), a unique functional relation can be established between the distributional properties of R_r (i.e., distribution, statistical moments, and achievable reliability) and h because $R_{c,\max}$, as shown in Equation (4), is a function of h.

However, this unique relation for substrate depth h, target retention ratio $R_{r,T}$, and achievable reliability $AR(R_{r,T};\ h)$, defined by Equation (22), would not exist when model parameters describing the rainfall-runoff transformation processes are subject to epistemic uncertainties. Under such circumstance, treating model parameters that characterize soil, plant, and climatic properties as deterministic constants would render a GR design not achieving the target performance with desired confidence. In the following section, an analysis framework is presented to treat the epistemic uncertainties imbedded in the AP GR model and to incorporate their effects in the evaluation and design of the GR systems.

INCORPORATING EPISTEMIC UNCERTAINTY IN THE AP GR MODEL

To quantify the overall uncertainty of the GR model, the parameters subject to epistemic uncertainty, in addition to aleatory ones, that affect probabilistic features of GR performance (such as V_{rg}, R_r, and AR) should also be analyzed. In this study, the five model parameters subject to epistemic uncertainties are θ_{fc}, θ_{wp}, S_l, E_a, and initial solid moisture ratio, C_i. Their effects on the retention performance of a GR system are briefly described. Uncertainty features of these model parameters appeared in the literature are collected and analyzed in this section. The procedures to incorporate epistemic uncertainty are outlined in Stage-II of Figure 1.

Epistemic uncertainties in GR model parameters

Field capacity and wilting point of the substrate

The substrate in GR establishment provides water, nutrients, and physical sustentation to vegetation. Among the physical properties of the GR substrate, field capacity and wilting point are the two key players affecting substrate's *WHC*. Field capacity θ_{fc} indicates substrate's ability to retain water against gravitational pull (DeNardo *et al.* 2005). Bengtsson (2005) showed that runoff from GR occurs when soil moisture content reaches θ_{fc}. Wilting point θ_{wp} is the soil water content that is held so tightly by the soil matrix that cannot be extracted by roots. It mainly depends upon the soil moisture profile, root distribution, plant transpiration rate, and temperature (Taylor & Ashcroft 1972).

In GR establishments, engineered substrates are often used. When commercial substrates are not available or too costly, substrates from locally available materials such as pasture soils or top soils are used (Brenneisen 2006; Dusza *et al.* 2017; Gong *et al.* 2018). Like most construction materials, within the properties of the GR substrate (engineered or natural) there exist some degree of variation due to the heterogeneity of the substrate in its production and installation. In a study to compare the consistency of measuring substrate physical properties by three standard test methods in Germany, USA, and Australia, Conn *et al.* (2020) show that, with replicate of soil samples, not only different test methods might produce inconsistent test results but also each standard test method yielded some variation of substrate properties.

In general, engineered substrates are more homogeneous, and therefore, their properties have narrower range of variation than those of natural substrates. For natural soils, Taylor & Ashcroft (1972, p. 300) present a diagram showing the range of values for θ_{fc}. Raghuwanshi & Mailapalli (2017, p. 144-2) provided a typical range of θ_{fc} and θ_{wp} for different types of natural soils; some of which are found in the literature for the GR substrate. In a study of predicting soil *WHC* in terms of $(\theta_{fc} - \theta_{wp})$ over Korea, Hong *et al.* (2013) provided the statistical features (i.e., mean and standard deviation) of θ_{fc} and θ_{wp} of different natural soils. For natural soils that are found in use for GR substrates, i.e., sand, sandy loam, and loam, data listed in

Raghuwanshi & Mailapalli (2017) indicate that θ_{fc} has variation of 33.3, 28.6, 18.0%, respectively, whereas θ_{wp} has variation of 53.8, 33.3, 21.4%, respectively. For engineered or natural substrates used in GRs, information about the variation of θ_{fc} and θ_{wp} is relatively scarce. The great majority of the literature and commercial substrate specifications reports only the averaged or nominal values of substrate properties without offering the information about their ranges of variation. To assess the uncertainty features of θ_{fc} and θ_{wp}, it is advisable to test some substrate samples used in GR installation. The practice of repeated measuring of soil samples is sometimes found in GR studies, mostly involving laboratory experiments.

In the GR literature, very few studies directly report the magnitude of uncertainty of θ_{fc} and θ_{wp}, while most show variation of *WHC* of substrate used. Young (2014) investigated the substrate in three prototype GRs in Sheffield, UK in that several test sites in each GR installation were selected and six soil samples in each test site were analyzed. The average values *WHC* for the substrates at the three GR installations range from 0.359 to 0.590 with standard errors varying from ±0.12 to ±0.43. In a simulation study by Soulis *et al.* (2017) on GR test beds, a replica of three samples of the artificial substrate used yields a mean *WHC* of 0.542 with a standard error of ±0.0165. In the study of Dusza *et al.* (2017) on multi-functionality of the GR plant and substrate, five samples of two different substrates yielded an average *WHC* of 0.33 for natural sandy-loam soil and 0.41 for artificial substrate, with standard errors of ±0.213 and ±0.299, respectively.

Since the standard errors associated with the mean θ_{fc} and θ_{wp} of the substrate samples were not directly reported, a backward statistical analysis is made to estimate the coefficient of variation (*Cv*) of field capacity in test substrate samples. Based on the relation of $WHC = \theta_{fc} - \theta_{wp}$, by assuming (i) $Cv(\theta_{fc}) \cong Cv(\theta_{wp})$ and (ii) $\text{Mean}(\theta_{fc}) \gg \text{Mean}(\theta_{wp})$, the coefficient of variation of θ_{fc} can be estimated as $Cv(\theta_c) = \sqrt{n} \times [SE(\overline{WHC})/\overline{WHC}]$, in which n is the soil sample size, $SE(\overline{WHC})$ is the standard error of average *WHC*, $\overline{WHC}$.

The results of the backward analysis yielded an estimation of the coefficient of variation of field capacity in substrate samples of 8.2–17.4% for the three GR installations in Young (2014); 5.3% for the artificial substrate sample in Soulis *et al.* (2017); and 14.3 and 16.3% for natural and artificial substrates, respectively, in Dusza *et al.* (2017). Unlike the great majority of commercial GR substrates only list nominal value of *WHC*, it is interesting to find a company 'Ferm-O-Feed' in the Netherlands, which shows the *WHC* of its basic substrates for extensive GR is in the range of 0.30–0.50. This reveals a ±0.1 variation for *WHC* for the substrate. Compared with the variation of field capacity and wilting point in soils occurred in nature (Hong *et al.* 2013; Raghuwanshi & Mailapalli 2017), the magnitude of the variation of properties of engineered or laboratory-made substrates is smaller, but not negligible.

Interception

The overall retention of GR systems is a combination of plant interception, internal storage capacity of the vegetation, and storage capacity of the substrate, among which the majority of the storage capacity is provided by the substrate (Martin 2008; Stovin *et al.* 2015; Fryer 2017a). Having said that, Martin (2008) noted that, under a smaller rainfall event, the effect of interception loss S_l on GR systems cannot be ignored. Interception amount during a storm event may vary due to variations in vegetation type, density, and canopy covers. Some quantifications of interception for vegetation used in GR can be found in the literature. For example, Soulis *et al.* (2017) found interception for sedum ranges in 0.5–6.1 mm; Carter & Jackson (2007) used 3.1 mm based on urban forest. However, very few reports exist in the literature about the uncertainty of interception. To authors' limited understanding, the study by Fryer (2017a, 2017b) is the only one providing information on the variation of interception of two plant types in GR. Her laboratory measurements showed that interception for sedum has about 15% variation and 30% for meadow grasses. The 30% variation of interception for natural meadow grasses happens to be close to the study by Miralles *et al.* (2010) for event-based interception on a global scale, which reported an estimation of S_l ranging with 1.2 ± 0.4 mm.

ET rate

ET rate E_a encompasses the integral effect of soil, plant, and climatic components in a GR system. In general, *in situ* measurement of ET by instruments is costly and valid data for actual ET are difficult to obtain directly (Zhao *et al.* 2013). Alternatively, suitable empirical and semi-empirical models are often used to indirectly estimate ET by relating it to environmental factors (such as air temperature, relative humidity, solar radiation, and wind speed). Among others, potential ET models commonly found in GR applications are Penman–Monteith equation, Thornthwaite equation, Hargreaves equation, and Priestley–Taylor equation. Marasco *et al.* (2014) measured the hourly E_a at two extensive GRs in New York by the dynamic chamber method and compared the measured ET values with two ET estimation methods. They observed that the Penman-based method was better than the energy balance method. A literature review by Feng (2018) on ET values of green infrastructure reported that the ET rate of GRs generally falls within 0.003–11.38 mm/day. Ebrahimian *et al.* (2019) also provided a review concerning ET on runoff retention of green stormwater infrastructure and reported that the range of ET rate for pilot-scale GRs has a narrower range of 0.5–3.5 mm/day. Through literature review, Ebrahimian *et al.* (2019) also concluded that none of the available ET predictive equations, primarily derived for agricultural applications, do not accurately match observed ET data for GRs and rain gardens.

Note that the above-reported variations for GR ET are obtained from different locations of varying climatic conditions and vegetation. Therefore, they are not suitable for direct use for the uncertainty of ET at a given GR site. For *in situ* uncertainty quantification by any ET semi-empirical equations, measure error and random variation of model inputs/parameters reflecting local environmental conditions should be used. Although there are reports of GRs ET rates as mentioned above, information on the associated uncertainty is lacking. Nichols *et al.* (2004) applied the error propagation method to quantify the uncertainty of potential ET in the semi-arid region in New Mexico by three models, and the results are Penman 13%, Preistley–Taylor 18%, and Penman–Monteith 10%. McMahon *et al.* (2013) compared eight potential ET models and summarized their variations of estimation. Following ISO 'Guides to the expression of Uncertainty in Measurement' (ISO 2010), Chen *et al.* (2018) quantified the uncertainty of ET prediction associated with two equations for indoor cultivation due to inaccuracy of sensor measurements of environmental variables. Their examples showed that inaccuracy in sensor measurements could result in 8.4 and 17.3% of uncertainty in model-based ET prediction. Talebmorad *et al.* (2020) applied the bootstrap method, based on 55 years of climatic data at synoptic station in Isfahan, Iran, to evaluate the uncertainty of the mean and variance of monthly reference crop ET estimated by FAO-56 Penman–Monteith and Hargreaves–Samani models. The ranges of the variation of estimated mean monthly ET values are 0.228–0.786 mm/day by FAO-56 Penman–Monteith equation and 0.176–0.362 mm/day by Hargreaves–Samani equation, which are equivalent to 6.9–28.2% by the former equation and 5.0–14.9% by the latter. These ranges of variation in monthly ET estimate are attributed to uncertainty in climatic inputs/parameters to prediction equations. UA approaches cited above and others can be applied to quantify ET rate uncertainty when typical vegetation types in GRs are used.

Initial soil moisture

In the above AP GR model, Equations (8)–(11), the evapotranspirable water amount W_i depends on the initial soil moisture θ_i of substrate and other system parameters as:

$$W_i = \begin{cases} R_{c,\max}, & \text{if } V \geq S_l + S_c + (\theta_{fc} - \theta_i)h \\ V + (\theta_i - \theta_{wp})h, & \text{otherwise} \end{cases} \tag{23}$$

in which the value of θ_i should be bounded in $[\theta_{wp},\ \theta_{fc}]$. In this study, θ_i is represented by the initial soil moisture ratio $C_i = (\theta_i/\theta_{fc})$ and treated as one of the model parameters. Since θ_i largely depends on the rainfall characteristics, substrate properties, and climatic factors, its value could be highly variable from one rainfall event to another. Physically, C_i is bounded within $[(\theta_{wp}/\theta_{fc}),\ 1]$ of which the lower bound of the bounding interval depends on two soil moisture characteristics subject to uncertainty.

Method of UA

When a design is based on model outputs that, in turn, are functions of several model parameters with uncertainty, the design problem becomes decision-making under uncertainty. Quantifying information about the uncertainty features of model outputs on which the design is affected is the objective of UA.

Methods of varying levels of sophistication have been developed and used for UA. They can broadly be classified into analytical methods and approximated methods. The former can directly derive the probability distribution and/or statistical moments of model outputs from those of random model parameters. The latter estimate the statistical features of model outputs through model evaluation at selected sampling points in the parameter space. Different approximated methods choose different sets of sampling points according to their theoretical considerations. The analytical methods, although mathematically elegant, are restrictive in their applications to practical problems. Several approximated methods (such as the first-order variance estimation method, probabilistic point estimation methods, and Monte Carlo simulation) are often used in UA of practical problems. Detailed descriptions of the various UA methods can be found elsewhere (Ayyub & Gupta 1998; Cacuci 2003; Tung & Yen 2005). Due to the complexity of the functional relation between the GR model parameters and concerned model output (e.g., aleatory-based retention performance reliability), a sampling-based method is adopted herein for UA.

Generating model input-output database

In this study, the Latin hypercube sampling (LHS) scheme (Iman & Helton 1988; McKay 1988) is used for establishing an input-output database of the probabilistic GR model for UA. The concerned model outputs herein are the achievable reliability $AR(R_{r,T},\ h|\boldsymbol{X})$ under a stipulated target retention ratio $R_{r,T}$ and substrate depths h as affected by the above-mentioned five model parameters subject to the uncertainty of epistemic nature, i.e., $\boldsymbol{X} = (\theta_{fc}, \theta_{wp}, S_l, E_a, C_i)$. The LHS scheme is chosen for its computational efficiency and accurate estimation of model outputs' statistical features.

LHS samples involving K independent random model parameters with sample size M can be generated by (Pebesma & Heuvelink 1999):

$$x_{km} = F_k^{-1}\left(\frac{s_{km} - u_{km}}{M}\right), \quad m = 1, 2, \ldots, M; \quad k = 1, 2, \ldots, K \tag{24}$$

where x_{km} is the mth generated random variate of the kth random variable X_k; $F_k^{-1}(\cdot)$ is the inverse CDF of the kth random variable; s_{km} is a random permutation of 1 to M for the kth random variable, X_k; and u_{km} is a uniform random variate in [0, 1], i.e., $u_{km} \sim U[0, 1]$. For a problem involving N concerned model outputs (e.g., achievable reliability of varying target retention ratios and substrate depths) and K random model parameters, an input-output database can be generated by the LHS scheme as:

$$(y_{1m},\ y_{2m},\ \ldots,\ y_{Nm}) = g(x_{1m},\ x_{2m},\ \ldots,\ x_{Km}), \quad m = 1,\ 2,\ \ldots,\ M \tag{25}$$

where $g(\cdot)$ is the representation of the model; $(y_{1m},\ y_{2m},\ \ldots,\ y_{Nm})$ is the vector of N model outputs obtained under the condition of K model parameters $(x_{1m},\ x_{2m},\ \ldots,\ x_{Km})$ in the mth LHS sample. Based on M sets of model outputs, $(y_{1m},\ y_{2m},\ \ldots,\ y_{Nm})_{m=1,2,\ldots,M}$, one can easily estimate the statistical features (e.g., distribution model and statistical moments) of the N concerned model outputs.

There are various applications of the LHS scheme to UA of hydrosystem engineering problems which include, but are not limited to, sediment transport modeling (Yeh & Tung 1993), water-quality modeling (Manache & Melching 2004), rainfall-runoff modeling (Yu et al. 2001; Christiaens & Feyen 2002), storm water best management practices (Park et al. 2011), dam overtopping (Goodarzi et al. 2013), water erosion prediction (Ascough et al. 2013), urban drainage modeling (Li et al. 2014), hydrological and sediment modeling (Shen et al. 2012), and surface and subsurface hydrologic simulations (Miller et al. 2017).

Quantification of the uncertainty of achievable reliability

To further improve the accuracy and stability in estimating the uncertainty features of the GR's achievable reliability, $AR(R_{r,T},\ h|\boldsymbol{X})$ in Equation (22), the LHS scheme, in conjunction with the antithetic variates (AV) technique, are utilized in this study for UA. The AV technique (Hammersley & Morton 1956) attains the goal of variance reduction by generating random variates that induce the negatively correlated quantity of interest between separate simulation runs.

By the AV technique, the statistical features (e.g., moments) of concerned output, Y, can be estimated by computing the arithmetic average of its two unbiased estimators as:

$$\hat{\Omega}_Y = \frac{1}{2}\,[\hat{\Omega}_Y(U') + \hat{\Omega}_Y(U'')] \quad (26)$$

in which, $\hat{\Omega}_Y$ is the estimator of the unknown statistical features, Ω_Y, of concerned model output Y; $\hat{\Omega}_Y(U')$, $\hat{\Omega}_Y(U'')$ are the unbiased estimators of the statistical features of model output Y based on random samples generated from two uniform random variates $U' \sim U[0, 1]$ and $U'' \sim U[0, 1]$, respectively. With $U'' = 1 - U'$, the two uniform random variables U' and U'' are negatively correlated, the two estimators $\hat{\Omega}_Y(U')$ and $\hat{\Omega}_Y(U'')$ would be unbiased, but negatively correlated estimators of Ω_Y. Then, the adopted estimator $\hat{\Omega}_Y$ by Equation (26) will have smaller variance than each individual estimator, $\hat{\Omega}_Y(U')$ and $\hat{\Omega}_Y(U'')$, for estimating the statistical quantity of concerned model output, Ω_Y.

Probabilistic GR design considering aleatory and epistemic uncertainties

According to Equation (22), $AR(R_{r,T},\ h|\boldsymbol{X})$ depends on the GR system parameters $\boldsymbol{X}$ that are subject to epistemic uncertainties. Hence, AR is also a quantity subject to uncertainty for any stipulated $R_{r,T}$ and h as schematically shown by the two distributions in Figure 2. Through UA, the statistical features of the GR performance indicator AR (such as its probability distribution and statistical moments) can be quantified and their functional relations with the $R_{r,T}$ and h established.

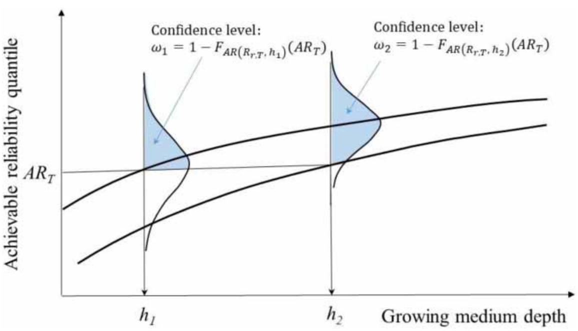

Figure 2 | Uncertainty of achievable reliability due to epistemic uncertainty in the GR model parameters.

Suppose that AR is a random variable having a CDF $F_{AR}(\vartheta_{AR})$, defined by its distributional parameters ϑ_{AR}. Because AR to meet a specified $R_{r,T}$ is uncertain, from design viewpoint, one would wish to determine the substrate depth h, such that the GR system can meet the target reliability AR_T with a specified confidence level ω. Referring to Figure 2, the GR system with h having confidence ω of meeting the desired $R_{r,T}$ and AR_T is the exceedance probability as shown by the shaded areas. The two solid curves in Figure 2 each represents confidence level, ω_1 and ω_2 ($\omega_2 > \omega_1$), respectively. As can be seen that, to maintain the same $R_{r,T}$ and AR_T with a higher confidence ω, one has to increase substrate depth h. In the context of design, considering aleatory and epistemic uncertainty simultaneously, the design substrate depth h_{dsgn} can be determined by solving the following equation:

$$\begin{aligned}\omega_{dsgn} &= Pr\{AR(R_{r,T}, h_{dsgn}) \geq AR_T|\vartheta_{AR}\} \\ &= 1 - F_{AR(R_{r,T},h_{dsgn})}\{AR_T|\vartheta_{AR}\}\end{aligned} \quad (27)$$

where ω_{dsgn} is the desired confidence level; $F_{AR(R_{r,T},h_{dsgn})}\{AR_T|\vartheta_{AR}\}$ is the CDF of random $AR(R_{r,T}, h_{dsgn})$.

Since the value of AR is bounded between 0 and 1, it is reasonable to postulate that the AR follows a standard Beta distribution, i.e., $AR \sim f_{Beta}(\mu_{AR}, \sigma_{AR})$, with its mean and standard deviation that are related to $R_{r,T}$ and h. Namely, $\mu_{AR}(R_{t,T}, h)$ and $\sigma_{AR}(R_{t,T}, h)$ can be explicitly expressed in terms of $R_{r,T}$ and h. Under the condition of standard Beta distribution for AR, the design substrate depth h_{dsgn} having design confidence ω_{dsgn} of meeting $R_{r,T}$ and AR_T can be determined by solving:

$$F_{AR(R_{r,T},\, h_{dsgn})}\{AR_T|\vartheta_{AR}\} = 1 - \omega_{dsgn} \quad (28)$$

in which, $F_{AR(R_{r,T},\, h_{dsgn})}\{AR_T|\vartheta_{AR}\}$ is the CDF of random AR.

ILLUSTRATION

To illustrate the probabilistic performance of an extensive GR system considering aleatory and epistemic uncertainty, data used in Zhang & Guo (2013) are adopted herein. The two rainfall properties at Metro International Airport

Table 1 | Statistical properties of uncertain factors in the example extensive GR

(a) Model inputs subject to aleatory uncertainty				
Rainfall event amount, V			Dry period between rainfall events, B	
$E(V) = 14.35$ mm (Exponential)			$E(B) = 97.95$ h (Exponential)	
(b) Model parameters subject to epistemic uncertainty				
ET rate, E_a (mm/h)	Field capacity, θ_c	Wilting point, θ_{wp}	Interception loss, S_l (mm)	Initial soil moisture ratio, C_i
$0.11 \pm 25\%$ (Uniform)	$0.232 \pm 15\%$ (Uniform)	$0.116 \pm 20\%$ (Uniform)	$2 \pm 30\%$ (Uniform)	0.5–1 (Uniform)

Note: ±% value defines the range of variation about the mean value.

Station in Detroit from April 1 through October 31 have been tested to follow exponential distributions with the mean values listed in Table 1(a). The substrate of the GR system is made of loamy soil, and the values of soil, plant, and climatic parameters listed in Table 1(b), according to Zhang & Guo (2013), are taken to be the mean values. As the initial soil moisture ratio C_i is bounded within the interval of $[(\theta_{wp}/\theta_{fc}),\ 1]$, without monitored data available, the range of variation of C_i is set in [0.5, 1] in which the lower bound is determined by the ratio of the mean values of θ_{wp} and θ_{fc} for illustration purposes. Without losing generality, uniform distribution, which corresponds to maximum entropy in comparison with other unimodal distributions, is adopted herein for each random model parameter. Furthermore, the five model parameters in Table 1(b) are treated to be independent random variables, and their ranges of variation are consulted from the data in the literature presented in the 'Epistemic uncertainties in GR model parameters' section only for illustration purposes.

To quantify model parameter uncertainty that reflects the on-site condition, it is desirable to analyze the variation of local climatic variables and conduct tests on limited *in situ* GR substrate samples. It should also be noted that the statistical features of retention ratio (e.g., mean value and achievable reliability) presented in this example should be referenced to the period of analysis of rainfall record (i.e., April–October in this example).

Behavior of the AP GR model

By considering the AP GR model, this section examines the statistical features of R_r according to the derived analytical expressions in the 'AP GR Model' section. To facilitate the illustration and discussion, data for the mean values of model parameters in Table 1 are used.

Distribution of retention ratio

The PDF and CDF (Equations (10) and (11)) of R_r under $W_i = R_{c,\max}$ are shown in Figure 3, respectively. These two figures clearly show that R_r is a random variable with discontinuity at $R_r = 1$ where the GR produces no runoff. As the substrate depth increases, the probability of producing zero runoff at $R_r = 1$ gets higher and the curve corresponding to $0 \leq R_r < 1$ drops lower as shown in Figure 3.

For a fixed substrate depth, $h = 100$ mm, Figure 4 shows a comparison of the exceedance probability (1-CDF) of R_r under the conservative and optimistic conditions of evapotranspirable water. With regard to rainwater retention performance, $W_i = R_{c,\max}$ represents the conservative scenario, whereby more water in the substrate is available for ET during the dry period. Under such circumstance, the available *WHC* in the substrate to accommodate the incoming rainfall would be less, so is the corresponding R_r. Hence, the likelihood that the GR system to have R_r exceeding a stipulated value would be lower than that of under the optimistic condition of $W_i = 0$.

Statistical moments of retention ratio

Figure 5 shows the variations of mean and standard deviation of R_r with substrate depth under conservative and optimistic values of W_i. The mean R_r (the two blue lines) increases with substrate depth because available *WHC* of the substrate becomes larger. Also, the rate of increase in mean R_r is decreasing with substrate depth.

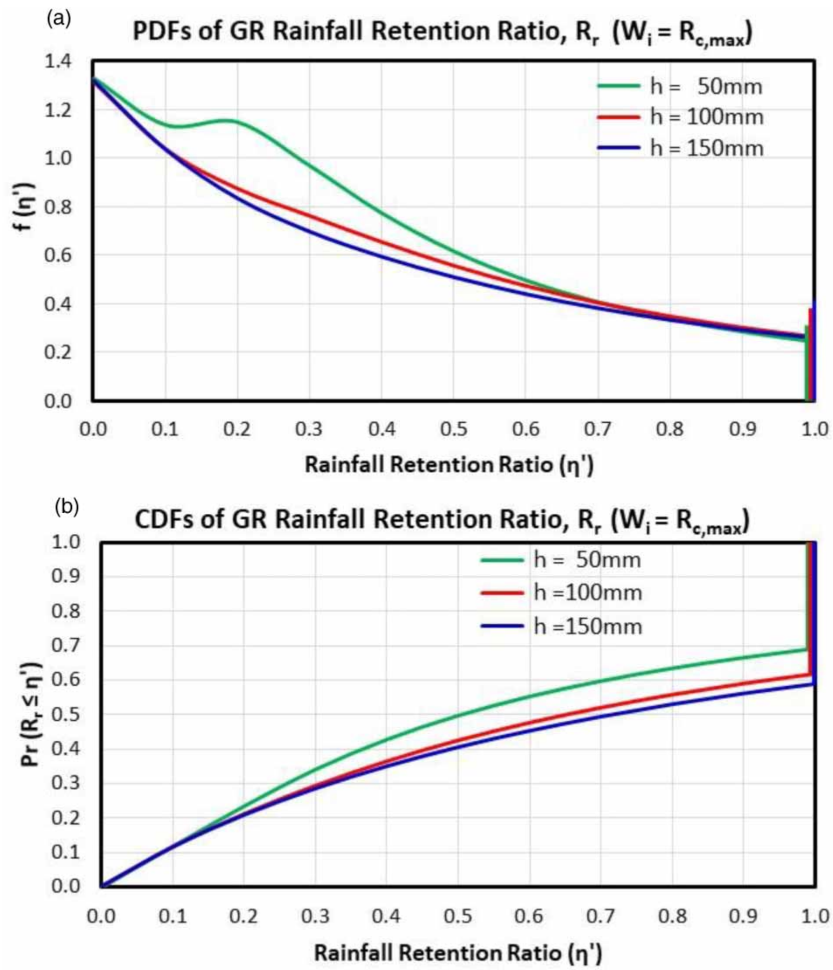

Figure 3 | (a and b) PDF and CDF of R_r of different substrate depths under $W_i = R_{c,\max}$.

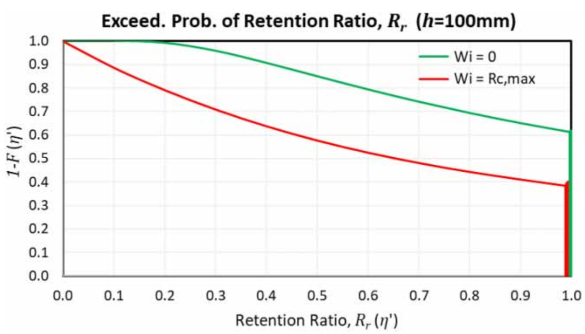

Figure 4 | Exceedance probability of R_r under conservative and optimistic W_i ($h = 100$ mm).

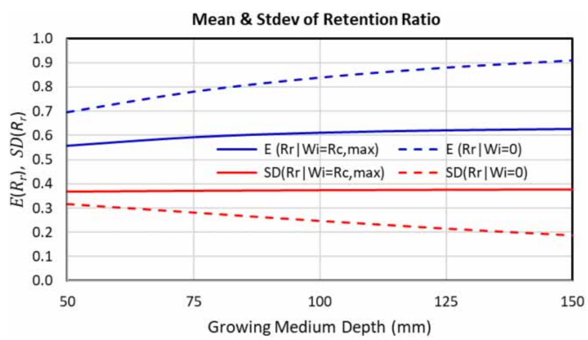

Figure 5 | Variation of mean and standard deviation with substrate depth of R_r under $W_i = R_{c,\max}$ and $W_i = 0$. Please refer to the online version of this paper to see this figure in colour: http://dx.doi.org/10.2166/nh.2020.086.

As for the standard deviation of R_r (the two red lines), Figure 5 reveals that the variability of R_r is lower when the value of W_i is smaller. The variability of retention ratio with substrate depth is fairly stable under $W_i = R_{c,\max}$, whereas it decreases with substrate depth under $W_i = 0$. This can be explained that with a low value of W_i, the corresponding initial soil moisture content at the beginning of the incoming rainfall event would be low and the available *WHC* of the substrate would be high to accommodate the rainfall event. The net effect would result in a higher mean and lower standard deviation of R_r.

As presented in the 'Statistical moments of retention ratio' section, the mean R_r can be estimated by several ways. Figure 6 shows a comparison of estimated mean R_r by the first-order method, Equation (13), the second-order method, Equation (14), and the analytical solution, Equation (19). In comparison with the analytical solution, Figure 6 shows that the first-order method significantly underestimate the mean R_r, whereas the second-order method, as expected, provides significant improvement with somewhat over-estimation as the substrate depth increases. This is because that the correlation between the rainfall amount and runoff volume plays an important role in estimating the mean R_r.

GR design using the AP model

Based on Equation (10), the CDF of R_r can be used to define a unique relationship for AR, substrate depth, h, and $R_{r,T}$ as shown in Figure 7, under the conservative condition $W_i = R_{c,\max}$. Clearly, for a given h, the AR of a GR system decreases with increase in $R_{r,T}$. For a specific $R_{r,T}$, the performance reliability increases with h. One can also see that by increasing h, the higher $R_{r,T}$ would be expected while maintaining AR at the same.

Since $W_i = R_{c,\max}$ corresponds to a conservative condition with possible minimum *WHC* in the substrate, Figure 7 defines the lower bound of $AR - R_{r,T} - h$ relationship for a given h. The upper $AR - R_{r,T} - h$ curve can be

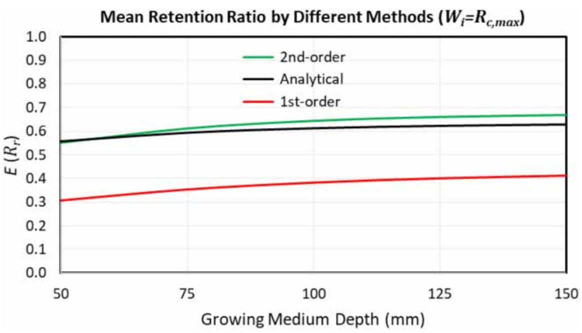

Figure 6 | Comparison of exact mean R_r with the first- and second-order approximations.

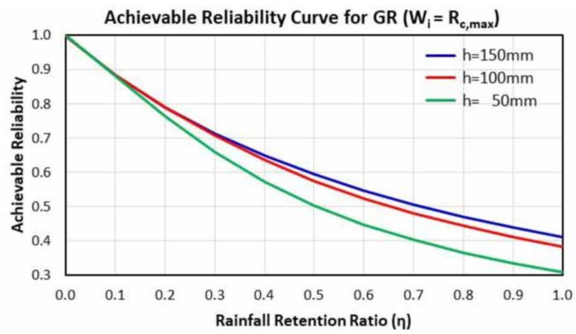

Figure 7 | $AR - R_{r,T} - h$ relations of the GR system under $W_i = R_{c,\max}$.

obtained under the optimistic condition of $W_i = 0$. Under the normal condition, the reliability would be somewhere between the two curves.

Uncertainty quantification of achievable reliability considering epistemic uncertainties

According to LHS samples of size 50, 100, 200, 300, 500, and 1,000 for the five GR model parameters in Equation (22), it was found that the estimated values of the first three statistical moments of AR did not satisfactorily converge, even under the sample size of 1,000. Hence, the AV technique for variance reduction is incorporated in the LHS scheme to enhance a stable and accurate estimation. As it turns out that the estimated statistical moments of AR from the AP GR model had a quick and satisfactory convergence with sample size of only 100.

To estimate the uncertainty features of $AR(R_{r,T}, h)$, random variates of the five parameters having epistemic uncertainty are generated by the LHS scheme jointly with the AV technique as:

$$\text{From } u': AR(R_{r,T}, h)'_m = g(E'_{a,m},\ \theta'_{fc,m},\ \theta'_{wp,m}, S'_{l,m},\ C'_{i,m}),\quad m = 1,\ 2,\ \ldots,\ M \tag{29}$$

$$\text{From } u'': AR(R_{r,T}, h)''_m = g(E''_{a,m},\ \theta''_{fc,m},\ \theta''_{wp,m}, S''_{l,m},\ C''_{i,m}),\quad m = 1,\ 2,\ \ldots,\ M \tag{30}$$

in which $u'' = 1 - u'$. The LHS/AV-based statistical properties of AR from the AP GR model can be computed according to Equation (26). For example, the raw moments of any order of $AR(R_{r,T}, h)$ by considering the epistemic uncertainty can be estimated by:

$$E[AR(R_{r,T}, h)^s] = \frac{1}{2}\{E[AR(R_{r,T}, h)'^s] + E[AR(R_{r,T}, h)''^s]\},\quad s = 1,\ 2,\ \ldots \tag{31}$$

where s is the order statistical moment; and

$$E[AR(R_{r,T}, h)''^s] = \frac{1}{M}\left\{\sum_{m=1}^{M}[AR(R_{r,T}, h)''_m]^s\right\};\quad E[AR(R_{r,T}, h)''^s] = \frac{1}{M}\left\{\sum_{m=1}^{M}[AR(R_{r,T}, h)''_m]^s\right\} \tag{32}$$

Then, the mean of LHS/AV-based estimator of $AR(R_{r,T}, h)$ can be estimated by Equation (31) with $s = 1$ and the variance with $s = 2$ as:

$$\sigma^2[AR(R_{r,T}, h)] = E[AR(R_{r,T}, h)^2] - E^2[AR(R_{r,T}, h)] \tag{33}$$

Other than the statistical moments, it is also important to assess its probability distribution of $AR(R_{r,T}, h)$ for reliability-based analysis and design of GR systems.

Statistical moments of $AR(R_{r,T},\ h, \boldsymbol{X})$

Based on 100 LHS/AV samples, Figures 7 and 8 show the mean and standard deviation of $AR(R_{r,T},\ h|\boldsymbol{X})$, respectively. As expected, Figure 8 reveals that the mean achievable reliability, $E_X[AR(R_{r,T},\ h|\boldsymbol{X})]$ increases with h, but decreases with $R_{r,T}$. The nominal values of $AR(R_{r,T},\ h|\boldsymbol{X} = \bar{\boldsymbol{x}})$ in Figure 8 are those obtained by using mean values of the model parameters $\bar{\boldsymbol{x}}$ listed in Table 1(b) without considering the epistemic uncertainties. It can be seen that the consideration of epistemic uncertainties yields slightly lower values of $E_X[AR(R_{r,T},\ h|\boldsymbol{X})]$ for thinner substrate depth, whereas for thicker substrate, the values of $E_X[AR(R_{r,T},\ h|\boldsymbol{X})]$ are higher than the nominal AR.

The standard deviation of achievable reliability, $SD_X[AR(R_{r,T},\ h|\boldsymbol{X})]$ also shows an increasing trend with the h (see Figure 9). However, the rate of increase is quite different under different $R_{r,T}$. For higher target retention ratio ($R_{r,T} = 0.7$ and 0.9), $SD_X[AR(R_{r,T},\ h|\boldsymbol{X})]$ monotonically increases with the substrate depth over the range of 50–150 mm, while under the lower target retention ratio ($R_{r,T} = 0.5$), $SD_X[AR(R_{r,T},\ h|\boldsymbol{X})]$ starts to drop slightly from the peak value (0.0614) at $h = 125$ mm to 0.0603 at $h = 150$ mm.

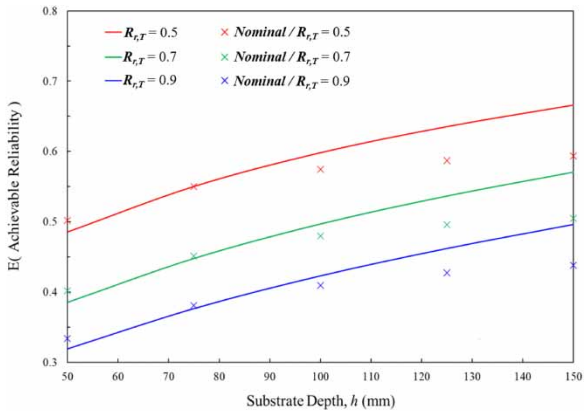

Figure 8 | Relation between $E_X[AR(R_{r,T},\ h|\boldsymbol{X})]$, $R_{r,T}$, and h.

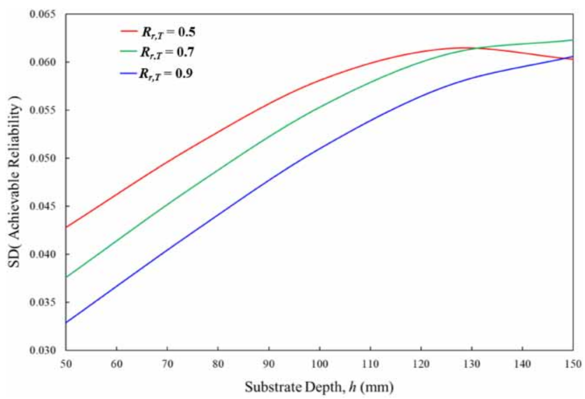

Figure 9 | Relation between $SD_X[AR(R_{r,T},\ h|\boldsymbol{X})]$, $R_{r,T}$, and h.

Distribution of $AR(R_{r,T},\ h|\boldsymbol{X})$

To identify a suitable distribution model for random $AR(R_{r,T},\ h|\boldsymbol{X})$ due to the presence of epistemic uncertainty, the chosen distribution model should reflect the properties of the collected data and could be validated through goodness-of-fit tests. In this study, 100 LHS/AV-generated random samples of $AR(R_{r,T},\ h)$ under different combinations of $R_{r,T}$ and h were tested for their goodness-of-fit to the standard Beta distribution. The standard Beta distribution was considered for being theoretically bounded in [0, 1] and versatile in shape. For illustration, Figure 10 shows the quantile–quantile (Q–Q) plot of sample values of $AR(R_{r,T},\ h)$ against the Beta-based quantiles under $R_{r,T} = 0.7$ and five substrate depths h. The data points closely follow the 45° line. Similar behavior of Q–Q plots are found for other combinations of $R_{r,T}$ and h. This indicates that the standard Beta distribution model is highly acceptable to describe the random behavior of $AR(R_{r,T},\ h|\boldsymbol{X})$ induced by model parameters with epistemic uncertainty. The Kolmogorov–Smirnov (KS) test was also used to formally examine the goodness-of-fit of the standard Beta distribution to AR sample data. The results reveal that the p-values range in (41.6, 98%), which are much higher than the commonly used significant level of 5%. Thus, the use of standard Beta distribution for random $AR(R_{r,T},\ h|\boldsymbol{X})$ is validated.

By adopting the standard Beta distribution for $AR(R_{r,T},\ h)$, one can determine the quantile values of achievable reliability as:

$$AR(q|R_{r,T},h) = F^{-1}_{S.Beta}\{q|E_X[AR(R_{r,T},h|\boldsymbol{X})], SD_X[AR(R_{r,T},h|\boldsymbol{X})]\} \tag{34}$$

where $AR(q|R_{r,T},\ h)$ is the qth-order quantile of uncertain $AR(R_{r,T},\ h)$; $F^{-1}_{S.Beta}[\cdot]$ is the inverse CDF of the standard Beta variable; $E_X[AR(R_{r,T},\ h|\boldsymbol{X})]$, $SD_X[AR(R_{r,T},\ h|\boldsymbol{X})]$ are the mean and standard deviation of $AR(R_{r,T},\ h)$, respectively, both are functions of $R_{r,T}$ and h. Figure 11 illustrates a series of quantile curves of achievable reliability under $R_{r,T} = 0.7$ and different h that can be established by Equation (34). One can also establish a confidence band of estimated $AR(R_{r,T},\ h)$. For instance, the 90% confidence band can be defined by using $q = 95\%$ quantile curve (blue solid line) as the upper bound and $q = 5\%$ quantile curve (blue dash line) as the lower bound. Figure 11 also shows that, without considering epistemic uncertainties, the nominal achievable reliability is slightly above the 50% quantile curve for shallow substrate and becomes lower than the 50% curve with thicker h. This means that, by considering only aleatory uncertainty, the use of substrate depth with $h \leq 75$ mm for an extensive GR, its corresponding nominal achievable reliability $AR(R_{r,T},\ h|\boldsymbol{X} = \bar{\boldsymbol{x}})$ to meet $R_{r,T} = 0.7$ has about 50% confidence. On the other hand, using thicker substrate depth with $h > 75$ mm, the confidence that the nominal achievable reliability to meet $R_{r,T} = 0.7$ is less than 50%. This means that the nominal achievable reliability of the system to meet the $R_{r,T}$ tends to be conservative because it underestimates the actual median achievable reliability. Furthermore, to maintain on the same level of non-exceedance probability, q, the required h to meet a $R_{r,T}$ would increase with achievable reliability.

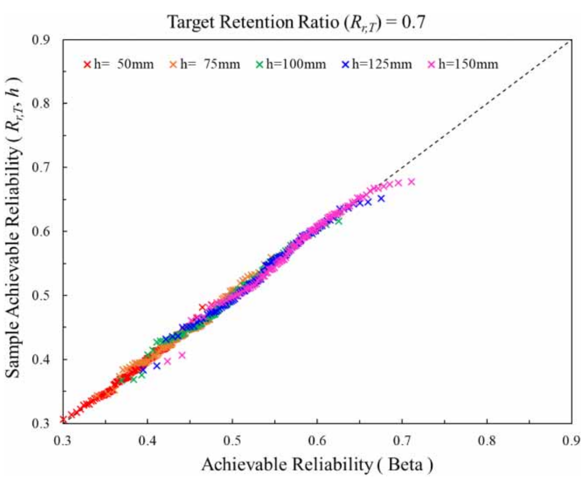

Figure 10 | Q–Q plot of LHS-based samples and beta-based achievable reliability.

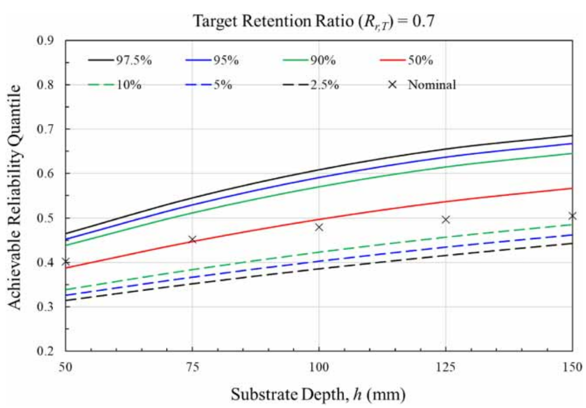

Figure 11 | Achievable reliability quantile curves for the GR system under $R_{r,T} = 0.7$ and different substrate depths. Please refer to the online version of this paper to see this figure in colour: http://dx.doi.org/10.2166/nh.2020.086.

Reliability-based GR design considering both aleatory and epistemic uncertainties

The reliability-based GR design requires the establishment of functional relationships between the statistical properties of standard Beta distribution and the two design parameters ($R_{r,T}$ and h). The two parameters of standard Beta distribution are related to the first two moments as:

$$\alpha_{AR} = (1-\mu_{AR})\left(\frac{\mu_{AR}}{\sigma_{AR}}\right)^2 - \mu_{AR} \tag{35}$$

$$\beta_{AR} = \mu_{AR}\left(\frac{1-\mu_{AR}}{\sigma_{AR}}\right)^2 - (1-\mu_{AR}) \tag{36}$$

in which α_{AR}, β_{AR} are the parameters of standard Beta distribution; μ_{AR}, σ_{AR} are the mean and standard deviation of $AR(R_{r,T}, h)$, respectively. Based on 100 LHS/AV-generated samples, the empirical functional relations between the mean μ_{AR} and standard deviation σ_{AR} of $AR(R_{r,T}, h)$ with $R_{r,T}$ and h are established, respectively, through regression analysis as:

$$\begin{aligned}\mu_{AR}(R_{t,T}, h) = {} & 0.7413 - 0.9883\, R_{t,T} + 0.0325\, h \\ & + 0.3871\, R_{r,T}^2 - 0.00079\, h^2 \\ & + 0.001659 R_{t,T}\, h\end{aligned} \tag{37}$$

$$\begin{aligned}\sigma_{AR}(R_{t,T}, h) = {} & 0.02573 + 0.004612\, h - 0.03304 R_{r,T}^2 \\ & - 0.000223 h^2 + 0.003187 R_{t,Th}\end{aligned} \tag{38}$$

In Equations (37) and (38), range of data in $R_{r,T}$ and h used are 0.4–0.9 and 5–15 cm, respectively. The coefficient of determination corresponding to the above two empirical equations are both 0.999. Utilizing Equations (37) and (38), the mean and standard deviation of $AR(R_{r,T}, h)$ for a pair of ($R_{r,T}$, h) can be computed which, in turn, can be used to determine the corresponding Beta distribution parameters defined by Equations (35) and (36). Then, the design substrate depth, h_{dsgn}, corresponding to $R_{r,T}$, AR_T, and design confidence, ω_{dsgn}, can be obtained by solving

$$F_{AR(R_{r,T},h)}\{AR_T \mid \alpha(AR|h_{dsgn}, R_{r,T}), \beta(AR|h_{dsgn}, R_{r,T})\} = 1 - \omega_{dsgn} \tag{39}$$

where $\alpha(\cdot)$ and $\beta(\cdot)$ are the parameters of standard Beta distribution describing random achievable reliability. The design confidence ω_{dsgn} is the probability that the random achievable reliability exceeds the stipulated target AR_T.

Figure 12 shows an example design diagram obtained from solving Equation (39) that defines the relationship between h_{dsgn} with confidence ω_{dsgn} to meet target $R_{r,T}$ and AR_T. It is clear that, for the fixed value of $R_{r,T}$, h_{dsgn} increases with ω_{dsgn} and AR_T.

CONCLUSION AND DISCUSSION

By considering the inherent randomness of rainfall amount of individual rainstorm event and inter-event dry period, this study extends the work of Zhang & Guo (2013) to derive the PDFs of the GR retention ratio R_r, based on which the analytical expression for the exact mean and variance of the retention ratio are derived. The analytical expression allows direct calculations of relevant statistical characteristics of R_r to rapidly assess the hydrological retention performance of a GR system without intensive simulation.

This study also evaluates the accuracy of estimating the mean R_r by two approximations with respect to the exact solution. The simplistic first-order approximation shows under-estimation of the true mean R_r. The second-order approximation significantly improves the first-order estimation because the variance of the rainfall amount and its correlation with the runoff volume play an important role.

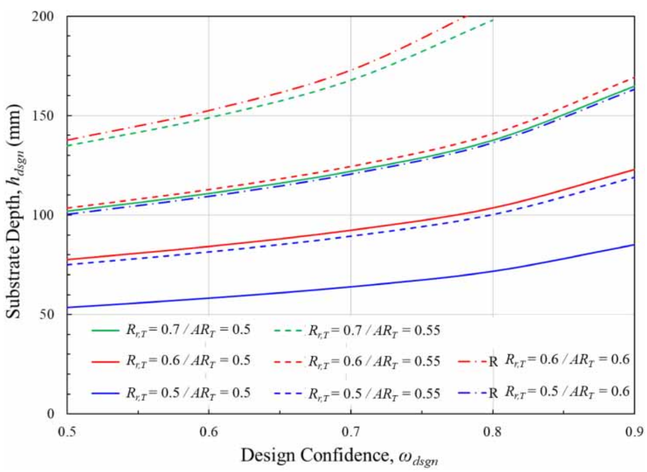

Figure 12 | Relationship between h_{dsgn} with ω_{dsgn} for meeting $R_{r,T}$ and AR_T.

Physically, runoff volume from a GR system is caused by rainfall, and therefore, the two random quantities should be positively correlated. This paper shows that such a correlation indeed is quite strong.

From the distribution function of random R_r, the relationship between target retention ratio $R_{r,T}$, achievable reliability AR, and substrate depth h for the AP GR model can be established. For illustration, the study shows a unique relation between the design substrate depth h_{dsgn} and AR. Nonetheless, there exists non-rain factors describing soil, plant, and climatic properties that affect the rainfall-runoff transformation process in the GR system. These non-rain factors are model parameters subject to the uncertainty of epistemic nature induced by knowledge deficiency. When epistemic uncertainty is taken into consideration, the AR obtained from the AP model is no longer certain. Thus, in order to have a comprehensive reliability assessment of the GR design, epistemic uncertainties are further incorporated in the AP model.

This study presents a systematic framework to assess the influence of the epistemic uncertainty on the performance of a GR system. Due to highly nonlinearity of the model parameter-output relations, the AV technique was jointly implemented with the LHS scheme in UA to obtain fast, stable, and accurate estimations of the statistical features of AR. Furthermore, the standard Beta distribution was found to fit the distribution of AR satisfactorily. One can easily construct the quantile curves and confidence intervals of AR according to its estimated moments from the LHS/AV procedure.

This study shows that the design of a GR system by considering only aleatory uncertainty due to the natural randomness of rainfall characteristics would roughly have 50% confidence to achieve the desired R_r. To determine a substrate depth for achieving the target reliability (AR_T) with 50% confidence or higher, when epistemic uncertainties are considered, one would have to use a thicker substrate depth h. The incremental depth beyond the nominal h (under aleatory uncertainty only) depends on the degree of epistemic uncertainty and the design confidence level (ω_{dsgn}). This incremental depth can be viewed as the safety margin to account for the presence of epistemic uncertainties. The proposed analysis framework leads to a more comprehensive and complete analysis/design of a GR system.

ACKNOWLEDGEMENTS

The study is supported by the Joint Research under the National Research Foundation (Korea)–Ministry of Science & Technology (Taiwan) Cooperative Program (MOST 105-2923-E-009-004-MY2). All data used in this paper are properly cited and referred to in the reference list.

DATA AVAILABILITY STATEMENT

All relevant data are included in the paper or its Supplementary Information.

REFERENCES

Abramowitz, M. & Stegun, I. 1964 *Handbook of Mathematical Functions with Formulas, Graphs, and Mathematical Tables*. Dover Publication Inc, New York, NY.

Adams, B. J., Fraser, H. G., Howard, C. D. D. & Hanafy, M. S. 1986 Meteorological data analysis for drainage system design. *J. Environ. Eng.* **112** (5), 827–848.

Allen, R. G., Pereira, L. S., Raes, D. & Smith, M. 1998 *Crop Evapotranspiration – Guidelines for Computing Crop Water Requirements*. Food and Agricultural Organization (FAO) of the United Nations, Rome, Italy.

Ascough II, J. C., Flanagan, D. C., Nearing, M. A. & Engel, B. A. 2013 Sensitivity and first-order/Monte Carlo uncertainty analysis of the WEPP hillslope erosion model. *Am. Soc. Agric. Biol. Eng.* **56** (2), 437–452.

Ayyub, B. M. & Gupta, M. M. 1998 *Uncertainty Analysis in Engineering and Sciences: Fuzzy Logic, Statistics, and Neural Network Approach*. Kluwer Academic Publishers, Dordrecht, The Netherlands.

Bengtsson, L. 2005 Peak flows from thin sedum-moss roof. *Nord. Hydrol.* **36**, 269–280.

Berndtsson, J. C. 2010 Green roof performance towards management of runoff water quantity and quality: a review. *Ecol. Eng.* **36**, 351–360.

Brenneisen, S. 2006 Space for urban wildlife: designing green roofs as habitats in Switzerland. *Urban Habitats* **4** (1), 27–36.

Cacuci, D. G. 2003 *Sensitivity and Uncertainty Analysis*. Chapman and Hall/CRC, Boca Raton, FL.

Carson, T. B., Marasco, D. E., Culligan, P. J. & McGillis, W. R. 2013 Hydrological performance of extensive green roofs in New York City: observations and multi-year modeling of three full-scale systems. *Environ. Res. Lett.* **8**, 024036.

Carter, T. L. & Jackson, C. R. 2007 Vegetated roofs for storm water management at multiple spatial scales. *Landscape Urban Plan.* **80** (1–2), 84–94.

Carter, T. L. & Rasmussen, T. C. 2006 Hydrologic behavior of vegetated roofs. *J. Am. Water Resour. Assoc.* **42**, 1261–1274.

Chai, C. T., Putuhena, F. J. & Selaman, O. S. 2017 A modelling study of the event-based retention performance of green roof under the hot-humid tropical climate in Kuching. *Water Sci. Tech.* **76** (11), 2988–2999.

Chen, L.-H., Chen, J. & Chen, C. 2018 Effect of environmental measurement uncertainty on prediction of evapotranspiration. *Atmosphere*. doi:10.3390/atmos9100400.

Chow, M. F., Abu Bakar, M. F., Sidek, L. M. & Basri, H. 2017 Effects of substrate types on runoff retention performance within the extensive green roofs. *J. Eng. Appl. Sci.* **12** (21), 5379–5383.

Christiaens, K. & Feyen, J. 2002 Use of sensitivity and uncertainty measures in distributed hydrological modeling with an application to the MIKE-SHE model. *Water Resour. Res.* **38** (9), 1169.

Cipolla, S. S., Maglionico, M. & Stojkov, I. 2016 A long-term hydrological modelling of an extensive green roof by means of SWMM. *Ecol. Eng.* **95**, 876–887.

Conn, R., Werdin, J., Rayner, J. & Farrell, C. 2020 Green roof substrate physical properties differ between standard laboratory tests due to differences in compaction. *J. Environ. Manage.* **261**, 110206.

DeNardo, J. C., Jarrett, A. R., Manbeck, H. B., Beattie, D. J. & Berghage, R. D. 2005 Stormwater mitigation and surface temperature reduction by green roofs. *Trans. ASAE* **48** (4), 1491–1496.

Der Kiureghian, A. & Ditlevsen, O. 2009 Aleatory or epistemic? Does it matter? *Struct. Saf.* **31**, 105–112.

Dusza, Y., Barot, S., Kraepiel, Y., Lata, J. C., Abbadie, L. & Raynaud, X. 2017 Multi-functionality is affected by interactions between green roof plant species, substrate depth, and substrate type. *Ecol. Evol.* **7**, 2357–2369.

Eagleson, P. S. 1978 Climate, soil, and vegetation, 2. The distribution of annual precipitation derived from observed storm sequences. *Water Resour. Res.* **14** (5), 713–721.

Ebrahimian, A., Wadzuk, B. & Traver, R. 2019 Evapotranspiration in green stormwater infrastructure systems. *Sci. Total Environ.* **688**, 797–810.

Ercolani, G., Chiaradia, E. A., Gandolfi, C., Castelli, F. & Masseroni, D. 2018 Evaluating performances of green roofs for stormwater runoff mitigation in a high flood risk urban catchment. *J. Hydrol.* **566**, 830–845.

Fassman, E. & Simcock, R. 2012 Moisture measurements as performance criteria for extensive living roof substrates. *J. Environ. Eng.* **138**, 841–851.

Feng, Y. 2018 Evapotranspiration from green infrastructure: benefit, measurement, and simulation. In: *Advanced Evapotranspiration Methods and Applications*. IntechOpen Publishing. http://doi.org/10.5772/intechopen.80910.

Fryer, M. 2017a *The Comparative Impacts of Meadow and Sedum Species on Green Roof Hydrology*. *MS Thesis*, Department of Civil Engineering, University of Toronto. 88 + viii pp.

Fryer, M. 2017b Evapotranspiration and interception by sedum and meadow species in green roof applications. In *Great Lakes and St. Lawrence Green Infrastructure Conference*, May 31–June 2, 2017, Detroit, Michigan.

Getter, K. L., Rowe, D. B. & Andresen, J. A. 2007 Quantifying the effect of slope on extensive green roof stormwater retention. *Ecol. Eng.* **31**, 225–231.

Gong, Y., Yin, D., Fang, X. & Li, J. 2018 Factors affecting runoff retention performance of extensive green roofs. *Water* **10**, 1217. doi:10.3390/w10091217.

Goodarzi, E., Shui, L. T. & Ziaei, M. 2013 Risk and uncertainty analysis for dam overtopping case study: the Doroudzan Dam, Iran. *J. Hydro. Environ. Res.* **8** (1), 50–61.

Guo, Y. 2001 Hydrologic design of urban flood control detention ponds. *J. Hydrol. Eng.* **6** (6), 472–479.

Guo, Y. 2016 Stochastic analysis of hydrologic operation of green roofs. *J. Hydrol. Eng.* **21** (7), 04016016.

Guo, Y. & Adams, B. J. 1998 Hydrologic analysis of urban catchments with event-based probabilistic models. I: Runoff volume. *Water Resour. Res.* **34** (12), 3421–3431.

Guo, Y. & Baetz, B. W. 2007 Sizing of rainwater storage units for green building applications. *J. Hydrol. Eng.* **12** (2), 197–205.

Guo, Y. P., Zhang, S. H. & Liu, S. G. 2014 Runoff reduction capabilities and irrigation requirements of green roofs. *Water Resour. Manage.* **28**, 1363–1378.

Hammersley, J. M. & Morton, K. W. 1956 A new Monte Carlo technique antithetic-variates. *Proc. Cambridge Phy. Soc.* **52**, 449–474.

Hong, S. Y., Minasny, B., Han, K. H., Kim, Y. & Lee, K. 2013 Predicting and mapping soil available water capacity in Korea. *Peer J.* **1**. doi:10.7717/peerj.71.

Hora, S. C. 1996 Aleatory and epistemic uncertainty in probability elicitation with an example from hazardous waste management. *Reliab. Eng. Syst. Saf.* **54**, 217–223.

Iman, R. L. & Helton, J. C. 1988 An investigation of uncertainty and sensitivity analysis techniques for computer models. *Risk Analy.* **8** (1), 71–90.

ISO/IEC 98-3. 2010 *Uncertainty of Measurement – Part 3: Guide to the Expression of Uncertainty in Measurement*. ISO, Geneva, Switzerland.

Johannessen, B. G., Muthanna, T. M. & Braskerud, B. C. 2018 Detention and retention behavior of four extensive green roofs in three Nordic climate zones. *Water* **10**, 671. doi:10.3390/w10060671.

Lambardi, A. M. 2017 *The Epistemic and Aleatory Uncertainties of the ETAS-Type Models: An Application to the Central Italy Seismicity*. Scientific Reports.

Li, Y. & Babcock Jr., R. W. 2014 Green roof hydrologic performance and modeling: a review. *Water Sci. Technol.* **69** (4), 727–738.

Li, C., Wang, W., Xiong, J. & Chen, P. 2014 Sensitivity analysis for urban drainage modeling using mutual information. *Entropy* **16**, 5738–5752.

Locatelli, L., Mark, O., Mikkelsen, P. S., Arnbjerg-Nielsen, K., Jensen, M. B. & Binning, P. J. 2014 Modelling of green roof hydrological performance for urban drainage applications. *J. Hydrol.* **519**, 3237–3248.

Manache, G. & Melching, C. S. 2004 Sensitivity analysis of a water-quality model using Latin hypercube sampling. *J. Water Resour. Plan. Manage.* **130** (3), 232–242.

Marasco, D., Hunter, B. N., Culligan, P. J., Gaffin, S. R. & McGillis, W. R. 2014 Quantifying evapotranspiration from urban green roofs: a comparison of chamber measurements with commonly used predictive methods. *Environ. Sci. Technol.* **48** (17), 10273–10281.

Martin, K. M. 2008 *The Dynamic Stormwater Response of a Green Roof*. MSc Thesis. University of Guelph, Ontario, CA.

McKay, M. D. 1988 Sensitivity and uncertainty analysis using a statistical sample of input values. In: *Uncertainty Analysis* (Y. Ronen, ed.). CRC Press, Boca Raton, FL.

McMahon, T. A., Peel, M., Lowe, C. L., Srikanthan, R. & McVicar, T. R. 2013 Estimating actual, potential, reference crop and pan evaporation using standard meteorological data: a pragmatic synthesis. *Hydrol. Earth Syst. Sci.* **17**, 1331–1363.

Miller, L. L., Berg, S. J., Davisona, J. H., Sudicky, E. A. & Forsyth, P. A. 2017 Efficient uncertainty quantification in fully-integrated surface and subsurface hydrologic simulations. *Adv. Water Resour.* **111**, 381–394.

Miralles, D. G., Gash, J. H., Holmes, T. R. H., De Jeu, R. A. M. & Dolman, A. J. 2010 Global canopy interception from satellite observations. *J. Geophys. Res.-Atmos.* **115**, D16122.

Mobilia, M., Longobardi, A. & Sartor, J. F. 2015 Green roofs hydrological performance under different climate conditions. *WSEAS Trans. Environ. Dev.* **11**, 264–271.

Mora-Melià, D., López-Aburto, C. S., Ballesteros-Pérez, P. & Muñoz-Velasco, P. 2018 Viability of green roofs as a flood mitigation element in the central region of Chile. *Sustainability* **10** (4), 1130.

Nichols, J., Eichinger, W., Cooper, D. I., Prueger, J. H., Hipps, L. E., Neale, C. M. U. & Bawazir, A. S. 2004 *Comparison of Evaporation Estimation Methods for a Riparian Area. IIHR Technical Report No 436, Hydroscience and Engineering*. University of Iowa, Iowa City, IA.

Park, D., Loftis, J. C. & Roesner, L. A. 2011 Performance modeling of storm water best management practices with uncertainty analysis. *J. Hydrol. Eng.* **16** (4), 332–344.

Pebesma, E. J. & Heuvelink, G. B. M. 1999 Latin hypercube sampling of Gaussian random fields. *Technometrics* **41** (4), 303–312.

Raghuwanshi, N. S. & Mailapalli, D. R. 2017 Ch.144 – Irrigation scheduling and management. In: *Handbook of Applied Hydrology*, 2nd edn. (V. P. Singh, ed.). McGraw-Hill, Inc., New York, NY.

Shen, Z. Y., Chen, L. & Chen, T. 2012 Analysis of parameter uncertainty in hydrological and sediment modeling using GLUE method: a case study of SWAT model applied to Three Gorges Reservoir Region, China. *Hydrol. Earth Syst. Sci.* **16**, 121–132.

Soulis, K. X., Valiantzas, J. D., Ntoulas, N., Kargas, G. & Nektarios, P. A. 2017 Simulation of green roof runoff under different substrate depths and vegetation covers by coupling a simple conceptual and a physically based hydrological model. *J. Environ. Manage.* **200**, 434–445.

Starry, O., Lea-Cox, J., Ristvey, A. & Cohan, S. 2016 Parameterization a water-balance model for predicting stormwater runoff from green roofs. *J. Hydrol. Eng.* **21** (12), 04016046.

Stovin, V., Poe, S. & Berretta, C. 2013 A modelling study of long-term green roof retention performance. *J. Environ. Manage.* **131**, 206–215.

Stovin, V., Poë, S., De-Ville, S. & Berretta, C. 2015 The influence of substrate and vegetation configuration on green roof hydrological performance. *Ecol. Eng.* **85**, 159–172.

Stovin, V., Vesuviano, G. & De-Ville, S. 2017 Defining green roof detention performance. *Urban Water J.* **14** (6), 574–588.

Talebmorad, H., Ahmadnejad, A., Eslamian, S., Ostad-Ali-Askari, K. & Singh, V. P. 2020 Evaluation of uncertainty in evapotranspiration values by FAO56-Penman-Monteith and Hargreaves-Samani methods. *Int. J. Hydrol. Sci. Tech.* **10** (2), 135–147.

Taylor, S. A. & Ashcroft, G. L. 1972 *Physical Edaphology: The Physics of Irrigated and Non-Irrigated Soils*. W.H. Freeman Publishing, San Francisco, CA.

Tung, Y. K. 2017 Effect of uncertainties on probabilistic-based design capacity of hydrosystems. *J. Hydrol.* **557**, 851–867.

Tung, Y. K. & Yen, B. C. 2005 *Hydrosystems Engineering Uncertainty Analysis*. McGraw-Hill Book Company, New York, NY.

Vijayaraghavan, K. 2016 Green roofs: a critical review on the role of components, benefits, limitations and trends. *Renew. Sustain. Energy Rev.* **57**, 740–752.

Yeh, K. C. & Tung, Y. K. 1993 Uncertainty and sensitivity of a pit migration model. *J. Hydraul. Eng.* **119** (2), 262–281.

Young, T. 2014 *The Influence of Green Roof Substrate Composition on Plant Growth and Physiological Health. PhD Thesis*, Department of Animal and Plant Science, the University of Sheffield, UK, September 2014. vii + 219 pp.

Yu, P. S., Yang, T. C. & Chen, S. J. 2001 Comparison of uncertainty analysis methods for a distributed rainfall-runoff model. *J. Hydrol.* **244**, 43–59.

Zhang, S. H. & Guo, Y. P. 2013 Analytical probabilistic model for evaluating the hydrologic performance of green roofs. *J. Hydrol. Eng.* **18** (1), 19–28.

Zhao, L. L., Xia, J. & Xu, C. Y. 2013 A review of evapotranspiration estimation methods in hydrological models. *J. Geog. Sci.* **68** (1), 127–136.

First received 17 June 2020; accepted in revised form 28 August 2020. Available online 14 October 2020